

Interchain coupling and localized vibration modes in conjugated polymers of finite length

Shi-jie Xie, Jian-Hua Wei, De-Sheng Liu, and Liang-Mo Mei
Department of Physics, Shandong University, Jinan, Shandong 250100, China

D. L. Lin

Department of Physics, State University of New York at Buffalo, Buffalo, New York 14260-1500
 (Received 1 May 1997)

The effects of interchain coupling on vibration modes localized around a polaron in polyacetylene of finite length are investigated. It is shown that the eight localized modes found in an isolated finite chain are delocalized between chains due to the interchain coupling. New modes of lattice vibration emerge because of the delocalization of the charged polaron. The well-known Goldstone zero-frequency mode becomes pinned by the chain ends for sufficiently short chains. Our results can qualitatively account for the frequency shifts observed recently in Raman scattering and infrared absorption spectra. [S0163-1829(97)04844-3]

I. INTRODUCTION

Extensive studies of nonlinear electron-phonon coupling systems in recent years have led to a good understanding of various excited states in quasi-one-dimensional conjugated polymers.^{1,2} Much of the electronic and optical properties in degenerate or nondegenerate conducting polymers are understood in terms of the low-lying excitations such as kinks, polarons, and bipolarons.²⁻⁶ Most of the early theoretical predictions are based on the one-dimensional model of isolated chains. The single-chain calculations yield good approximation in many cases as spinless electrical conductivity, dimerization amplitude, and optical absorption. This is because the interchain hopping energy is generally one order of magnitude smaller than that of the intrachain hopping.⁷

There are, however, also cases in which qualitative differences may result from the interchain coupling. For example, the parallel ordering bonds on neighboring chains⁸ is preferred because of the change of the interchain electron transfer,⁹ and the interchain coupling may provide the necessary binding for a stable bipolaron.¹⁰ On the other hand, it is shown on the molecular crystal model¹¹ that the interchain coupling is too strong in polyacetylene for a polaron to be stable.¹²⁻¹⁴ A more careful numerical study of an extended Su-Shrieffer-Heeger model¹⁵ then reveals that for both degenerate and nondegenerate conjugated polymers there exists a discontinuous change in the degree of delocalization at a critical value of the coupling strength.¹⁶ A polaron remains stable as long as the interchain coupling is smaller than the critical value t_i^c .

Very recently, a two-chain system with one- and two-bond random couplings was considered to study the electronic diffusion. It was found that a particular type of conducting band structure can explain the unusual transport properties of highly conducting polymers.¹⁷ Furthermore, a number of experiments on films of polyacetylene, polypyrrole, polythiophene, and polyaniline have indicated that interchain interactions and finite chain length have apparent effects on the electroluminescence and photoluminescence efficiencies of conducting polymers in light-emitting diodes.¹⁸⁻²¹

In realistic samples of herringbone structure, atomic displacements and energy levels resulting from adding an electron to a cluster of *t-PA* chains have been calculated for the tight-binding model.²² The work was later extended to include the coupling between chains of different lengths.²³ It was found that polarons stabilize only in long chains. If it is excited in a short chain, it will hop to a neighboring long chain provided that there exist interactions between the chains, even very weak ones. In the case of strong interchain coupling, the polaron delocalizes between chains. While the effect of interchain coupling on static polarons has been well studied, effects on the lattice vibration around a polaron remain open to investigation.

Vibration modes around a polaron in *t*-polyacetylene and around a bipolaron in polythiophene have been obtained for finite chains.^{24,25} Localized surface modes near free ends of the chain are found in these calculations and the results of Ref. 25 appear to be consistent with resonant Raman scattering experiments. A recent study of electronic absorption and vibration spectroscopy of doped polymers revealed that it is the polaron that is generated by doping in most nondegenerate conjugated polymers instead of the bipolaron, as has been generally believed.²⁶ Charged solitons or polarons in *t-PA* are important self-localized excitations, depending upon whether the number of carbon atoms in the chain is odd or even. It is therefore interesting to calculate vibration modes around a polaron in *t-PA* to help interpret Raman and infrared spectra.

We investigate in this paper effects of the interchain coupling on the localized vibration modes in finite chains. We consider two parallel *t-PA* chains with a charged polaron stimulated in one of them. It is found that the polaron is delocalized by increasing the coupling strength and at the same time localized vibration modes can be identified. The model Hamiltonian is given in Sec. II, where the scheme of a self-consistent calculation is also outlined. In Sec. III, we describe the results of our numerical computation and discuss the effects of interchain interactions.

II. THEORY

For the isolated *j*th chain, we assume the tight-binding SSH Hamiltonian

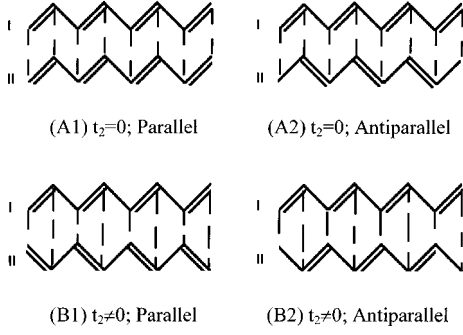


FIG. 1. Possible configurations for a pair of interacting chains, (A) $t_2=0$ and (B) $t_2\neq 0$.

$$\begin{aligned}
H_j = & - \sum_{n,s} [t_0 - \alpha(u_{j,n+1} - u_j)] (c_{j,n,s}^\dagger c_{j,n+1,s} + c_{j,n+1,s}^\dagger c_{j,n,s}) \\
& + \frac{1}{2} K \sum_n (u_{j,n+1} - u_{j,n})^2 + \frac{1}{2} M \sum_n u_{j,n}^2 \\
& + K' \sum_n (u_{j,n+1} - u_{j,n}), \quad (1)
\end{aligned}$$

where the notation is standard. The transverse vibration is not considered here because we are focusing on the interchain interactions. The last term in Eq. (1) is added to stabilize the free ends of the finite chain of N sites and $K' = -4\alpha/\pi$.²³ The interchain interaction is represented by the π -electron transfer integral perpendicular to the chain direction,¹⁹

$$H = - \sum_{n,s} t_\perp(n) (c_{1,n,s}^\dagger c_{2,n,s} + c_{2,n,s}^\dagger c_{1,n,s}), \quad (2)$$

where $t_\perp(n) = t_1 + (-1)^n t_2$ stands for the transfer integral between sites labeled by the same index n on two different chains. There are four possible configurations for a pair of identical chains, as shown in Fig. 1. When $t_2=0$, the interchain coupling $t=t_1$ is a constant and the dimerization in each chain is not independent, resulting in the configurations A1 and A2. The latter has lower energy according to calculations. When $t_2\neq 0$, the coupling between the pair of sites labeled by odd or even n is no longer the same. Numerical calculation shows that B1 has lower energy.

For a small deviation from the equilibrium configuration $\{u_{j,n}\}$, the vibration matrix is given by

$$\begin{aligned}
B_{i,j,m,n} = & \frac{2}{\pi\lambda} \delta_{i,j} (\delta_{m,n} \bar{\delta}_{m,1} + \delta_{m,n-1} \bar{\delta}_{m,N} + \delta_{m-1,n} \bar{\delta}_{m,1} \\
& + \delta_{m,n} \bar{\delta}_{m,N}) + 2(-1)^{m+n} \sum_{\mu,\nu}' \frac{c_{\mu\nu}^{im} c_{\mu\nu}^{jn}}{\epsilon_\mu - \epsilon_\nu}, \quad (3a)
\end{aligned}$$

$$\begin{aligned}
c_{\mu\nu}^{im} = & Z_{i,m,\mu} (Z_{i,m-1,\nu} \bar{\delta}_{m,1} - Z_{i,m+1,\nu} \bar{\delta}_{m,N}) \\
& + Z_{i,m,\nu} (Z_{i,m-1,\mu} \bar{\delta}_{m,1} - Z_{i,m+1,\mu} \bar{\delta}_{m,N}). \quad (3b)
\end{aligned}$$

The π -electron eigenvalues ϵ_μ and eigenstates $Z_{i,n,\mu}$ along with the static lattice configuration are determined self-consistently by the eigenequation

$$\begin{aligned}
& - \bar{\delta}_{n,1} [1 + (-1)^{n-1} (\phi_{i,n} + \phi_{i,n-1})] Z_{i,n-1,\mu} \\
& - \bar{\delta}_{n,N} [1 + (-1)^n (\phi_{i,n+1} + \phi_{i,n})] Z_{i,n+1,\mu} \\
& - \bar{\delta}_{i,j} [t_1 + (-1)^n t_2] Z_{j,n,\mu} = \epsilon_\mu Z_{i,n,\mu}, \quad (4)
\end{aligned}$$

and the static equilibrium condition

$$\phi_{i,n+1} + \phi_{i,n} = (-1)^n \pi\lambda \left(\sum_{\mu}' Z_{i,n+1,\mu} Z_{i,n,\mu} - \frac{2}{\pi} \right), \quad (5)$$

where we have introduced the order parameter $\phi_{in} = \alpha u_n / t_0$ and electron-phonon coupling constant $\lambda = 2\alpha^2 / \pi K t_0$, both of which are dimensionless. We have also defined $\bar{\delta}_{m,n} = 1 - \delta_{m,n}$ with the Kronecker delta $\delta_{m,n}$. The prime indicates summing over occupied electron states only and the spin index is neglected. The subscripts i, j label the chain and m, n label the site on each chain which has a total of N (CH) groups.

The calculation procedure is as follows. We first solve Eqs. (4) and (5) numerically for a given value of t . The iteration begins with a stimulated lattice configuration ϕ_{in} in each chain. The eigenvalues and eigenstates obtained from Eq. (4) are substituted in (5) to find a more stable configuration. The calculation is repeated with this new configuration. The criterion for self-consistency is that the difference between values of $\phi_{i,n+1} + \phi_{i,n}$ from two successive iterations is less than 10^{-5} . The resulting equilibrium configuration together with the electron eigenvalues and eigenstates is then substituted in Eq. (3a). All vibration modes can be found by diagonalizing the matrix $B_{i,j,m,n}$ and we only pick the localized ones for further investigation.

To study the effects of free ends, we consider chains of various lengths from 8 up to 120 (CH) groups. In this paper, the numerical work is carried out for t -PA with $\lambda = 0.24$. All energies are measured in units of t_0 , and frequencies in units of $(2/\pi\lambda)^{1/2} \omega_0$, where $\omega_0 = (4K/M)^{1/2}$ is the bare phonon frequency. We consider three cases with different coupling strengths between the two chains, that is, the weak coupling $t_\perp < 0.05$, intermediate coupling $0.05 < t_\perp < 0.1$ and strong coupling $t_\perp > 0.1$.

III. RESULTS AND DISCUSSION

For a single t -PA chain of infinite or finite length with periodic boundary conditions, we find eight localized vibration modes around an electron (or a hole) charged polaron. Figure 2 shows their vibration configurations. Two peculiar modes g_7 and g_8 known as staggered modes which do not exist in the continuous model appear here. They are apparently resulting from the discrete nature of the chain assumed in our calculation. g_1, g_4, g_6, g_8 are odd-parity modes and hence are infrared active, while g_2, g_3, g_5 , and g_7 , are even-parity modes and Raman active. A mode that has not, to our knowledge, been reported thus far is g_2' which is only weakly localized. It has the same parity as g_2 and its vibration structure including the frequency and configuration is also quite close to g_2 .

For short chains, the periodic boundary condition is no longer suitable. The free-end boundary condition introduced in Ref. 25 for the treatment of finite chains is now applied to

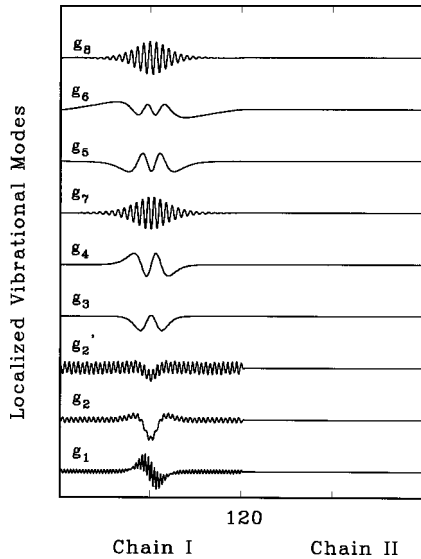


FIG. 2. Localized modes of lattice vibration in an isolated chain.

study the effects of chain ends on the vibration modes. It is found that the frequency of all modes depends on the chain length as is illustrated in Fig. 3. For nonstaggered modes, the frequency increases slowly with the decreasing chain length to $N \sim 40$. When the length decreases further, the frequency increases at a much faster rate. Of particular interest are the frequencies of modes g_7 and g_8 , which are relatively insensitive to the length change and vary little with the decreasing length. Moreover, we also find the enhancement of localization of vibration modes as the chain shortens except for g_7 and g_8 for which the localization is again insensitive to the variation of chain lengths.

To study effects of the interchain coupling, let us consider a negatively charged polaron initially stimulated in one chain. When the interchain interaction is turned on, the electric charge of the polaron begins to share between the two coupled chains. The amplitude of the original polaron decreases gradually and a secondary ‘‘polaron’’ with small amplitudes appears in the second chain. The process of charge transfer keeps going steadily with the increasing coupling

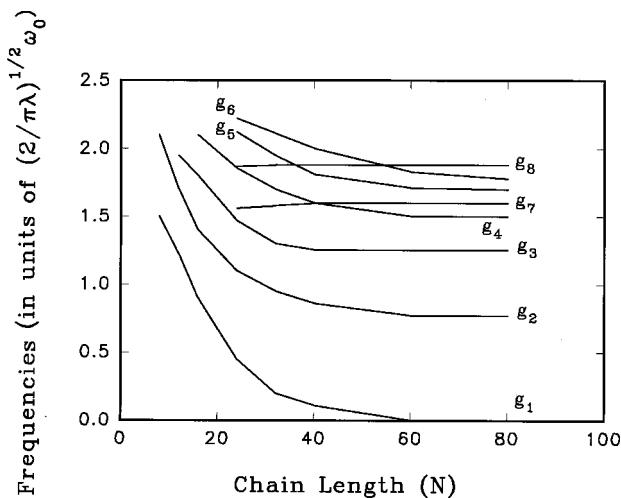


FIG. 3. Frequencies of localized vibration modes vs the chain length N .

TABLE I. Vibration frequency change due to the interchain interaction.

Localized mode	$t_{\perp}=0$	$t_{\perp}=0.025t_0$	$t_{\perp}=0.050t_0$
g_1	0	0	0
g_2	0.799	0.723	0.324
g_3	1.278	1.269	1.166
g_4	1.504	1.501	1.474
g_5	1.716	1.710	1.574
g_6	1.799	1.736	1.589
g_7	1.592	1.588	1.550
g_8	1.897	1.795	1.702
g'		1.796	1.739
g''		1.900	1.777
g'''			1.792
g''''			1.917

strength up to a critical value $t_{\perp}=t_{\perp}^c$. Then the system reaches a stable state in which the two ‘‘polarons’’ oscillate with the same amplitude and share equal charge. Further increase of the coupling then does not change the modes any more.

Because of the delocalization of a polaron between chains, the vibrational structure may change greatly. We first consider the interaction of various strengths between an antiparallel ordered ($t_2=0$) pair of identical chains with $N=120$. For cases of weak interchain coupling with $t_{\perp}=0.025t_0$ and $0.05t_0$, the polaron can maintain its integrity in the first chain with only a small fraction of charge transferred to the second. All eight modes around the polaron in the first chain still maintain their structures. Our calculation indicates, however, that localized vibration modes emerge in the second chain with a small amplitude for all nonstaggered modes. They result from the secondary charged ‘‘polaron’’ excited very weakly in this chain. On the other hand, the amplitudes and configurations of the g_7 and g_8 modes remain completely unchanged. Therefore, the interchain coupling has little influence on the staggered modes.

Vibration frequencies of all localized modes are found to decrease with increasing interchain coupling strength according to our calculation. Numerical results are shown in Table I. This is not difficult to understand because the interchain coupling delocalizes the polaron. It is also seen from the table that the higher the vibration frequency the smaller the resulting frequency shift is under the same coupling strength.

These results are consistent with recent observations.^{27,28} Frequency shifts in Raman spectra have been reported recently. From the observed Raman bands of a *PA* film heavily doped with SO_3 it is found that *p*-type (*n*-type) doping results in upshift (downshift) of phonon frequencies.²⁷ This may be understood as follows. The *p*-type doping supplies a hole in the chain, and the negatively charged acceptor between chains works against the possible electron exchange and hence tends to weaken the interchain coupling. Consequently, phonon frequencies upshift upon *p* doping, as we have seen from Table I. On the other hand, the *n*-type doping supplies an electron to the chain and the positive donor in the delocalized polaron between chains enhances electron exchange. Thus, *n*-type doping tends to strengthen the interchain coupling and downshifts phonon frequencies.

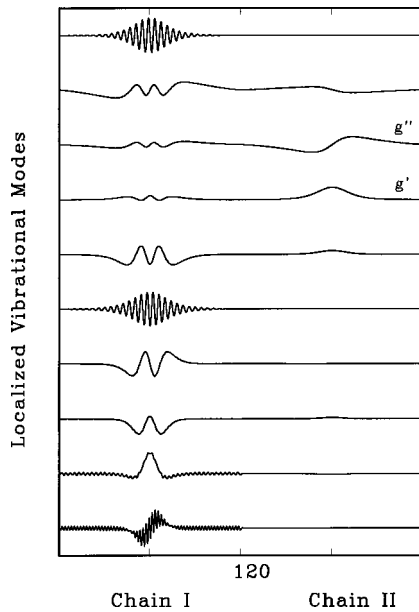


FIG. 4. Localized vibration modes in a pair of coupled chains with $t_{\perp} = 0.025t_0$ and $t_2 = 0$.

We believe that the interchain coupling is responsible for frequency upshifts observed in recent infrared absorption measurements of Durham-polyacetylene after long-time exposure in air. The observed upshifts of photoinduced infrared absorption peaks are attributed to (1) a charge transfer to oxygen absorbed and (2) chemical reaction of oxygen with the chain.²⁸ In our opinion, the oxygen atom absorbed works as a p -type doping which leads naturally to upshifts of phonon frequencies.

As illustrated in Figs. 4 and 5, the weak oscillations of the localized modes in the second chain are present but not

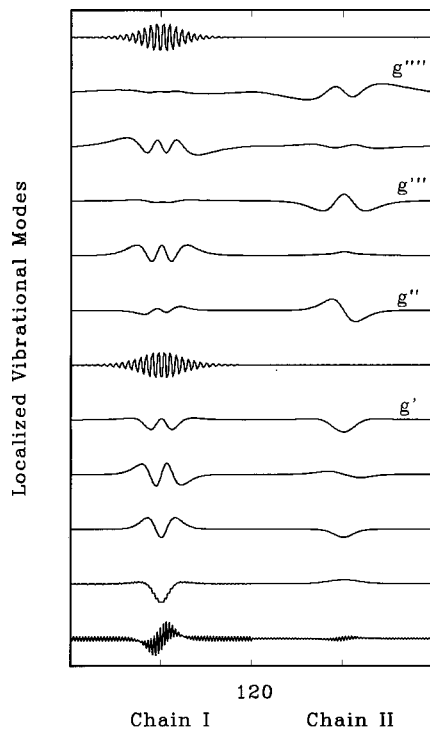


FIG. 5. Same as Fig. 4 except $t_{\perp} = 0.05t_0$ and $t_2 = 0$.

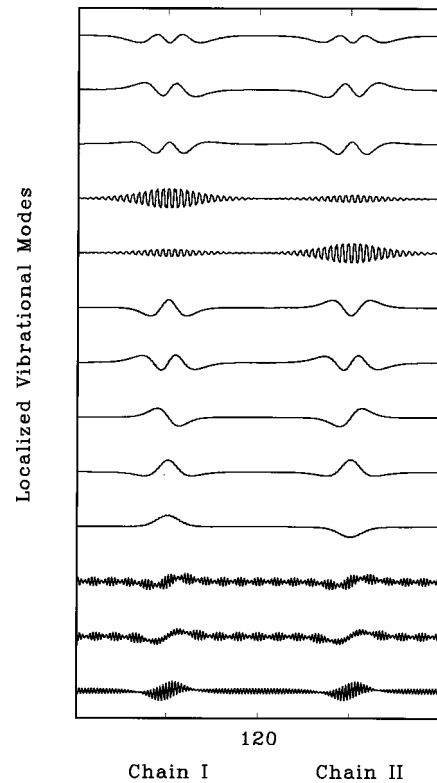


FIG. 6. Same as Fig. 4 except $t_{\perp} = 0.075t_0$ and $t_2 = 0$.

clearly seen in Fig. 4 because of the small interchain coupling, but they become observable in Fig. 5. It is also found from these figures that extra modes of localized vibration are created due to the coupling. For $t_{\perp} = 0.025t_0$, we find an even-parity mode g' at a frequency $\omega' = 1.796$ and an odd-parity mode g'' at $\omega'' = 1.900$, while four extra modes are excited for $t_{\perp} = 0.05t_0$, two even modes at $\omega' = 1.739$ and $\omega'' = 1.792$, and two odd modes at $\omega' = 1.777$ and $\omega'' = 1.917$. It is interesting to note that these extra modes all show larger amplitudes around the secondary polaron in the second chain than in the first chain.

For strong interchain coupling such as $t_{\perp} \geq 0.075$, the vibration frequency may change so much that modes can hardly be traced as more new modes are created. The results obtained for $t_{\perp} = 0.075t_0$ are shown in Fig. 6. The delocalization of polarons becomes apparent. The “polaron” in the first chain has a little more charge than that in the second according to the numerical results but cannot be easily seen in the figure. It is clear, however, that the staggered modes are still least affected by the interchain coupling.

When the coupling strength increases further, each chain has a polaron of the same charge of one half electron with equal amplitudes. The two chains become equivalent irrespective of the initial condition. Figure 7 shows the resulting 13 localized modes for $t_{\perp} = 0.10t_0$. The maximum amplitudes of each mode in both chains are equal. The localized configurations in two identical chains for each mode have the same parity, a property that does not depend on the strength of coupling. It is difficult to trace these modes back to their initial states in an isolated chain. Hence they are no longer labeled. On the other hand, there are still only two staggered modes that can easily be distinguished from others.

We now turn our attention to a pair of parallel ordering

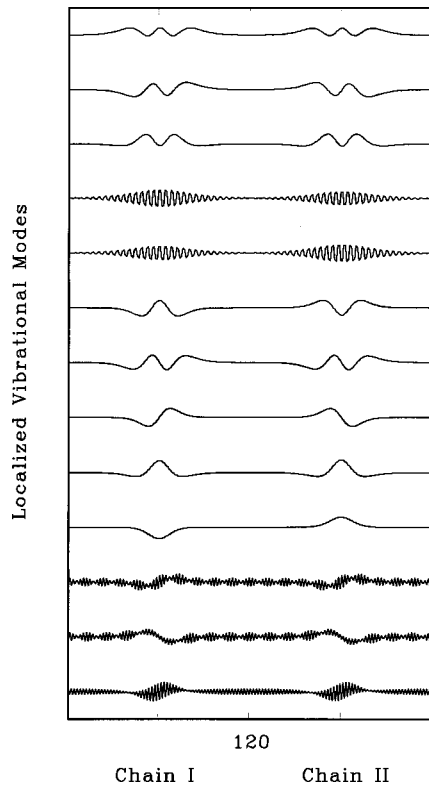


FIG. 7. Same as Fig. 4 except $t_1 = 0.10t_0$ and $t_2 = 0$.

chains with a charge polaron stimulated in one of them. When $t_2 \sim 0$, the results are found to be similar to what is discussed above. When $t_2 \neq 0$, we find more staggered modes emerging in the case of strong coupling. For example, localized mode for $t_2 = 1.5t_1$, and $t_1 \geq 0.075t_0$ are presented in

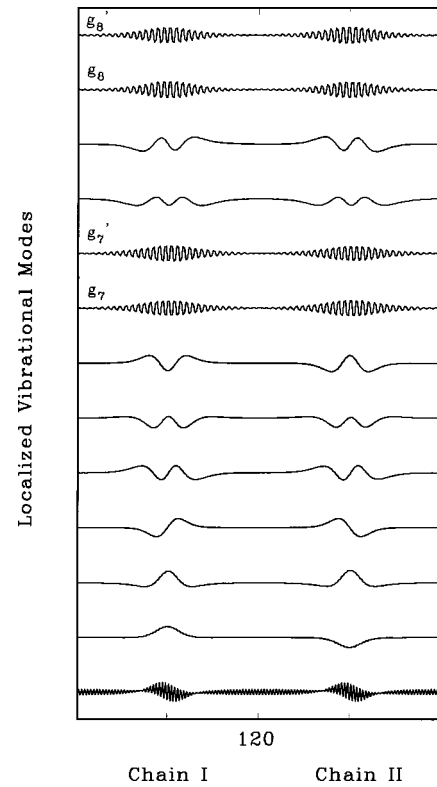


FIG. 8. Same as Fig. 4 except $t_1 = 0.075t_0$ and $t_2 = 1.50t_1$.

Fig. 8 in which four staggered modes are clearly identified, namely, two even-parity modes g_7 and g_7' and two odd-parity modes g_8 and g_8' . Thus, the configuration ordering of the two interacting chains determines the number and frequencies of the staggered modes.

- ¹See, for example, *Proceedings of the International Conference on the Physics and Chemistry of Low-Dimensional Synthetic Metals* [Mol. Cryst. Liq. Cryst. **117&118**, (1985)].
- ²A. J. Heeger, S. Kivelson, J. R. Schrieffer, and W. P. Su, Rev. Mod. Phys. **60**, 781 (1988).
- ³S. A. Brazovskii and N. N. Kirova, Pis'ma Zh. Eksp. Teor. Fiz. **33**, 6 (1981) [JETP Lett. **33**, 4 (1981)].
- ⁴A. R. Bishop, D. K. Campbell, and K. Fesser, Mol. Cryst. Liq. Cryst. **77**, 253 (1981).
- ⁵J. L. Bredas, R. R. Chance, and R. Silbey, Phys. Rev. B **26**, 5843 (1981); R. R. Chance, J. L. Bredas, and R. Silbey, *ibid.* **29**, 4491 (1984).
- ⁶S. J. Xie and L. M. Mei, J. Phys.: Condens. Matter **6**, 3909 (1994).
- ⁷S. Jeyadev and J. R. Schrieffer, Phys. Rev. B **30**, 3620 (1984).
- ⁸H. Kahlert, A. Leitner, and G. Leising, Synth. Met. **17**, 467 (1987).
- ⁹D. Bareriswyl and K. Maki, Phys. Rev. B **38**, 8135 (1988).
- ¹⁰J. A. Blackman and M. K. Sabra, Polymer **31**, 621 (1990).
- ¹¹T. Holstein, Ann. Phys. (N.Y.) **8**, 325 (1959).
- ¹²D. Emin, Phys. Rev. B **33**, 3973 (1986).
- ¹³Y. N. Gartstein and A. A. Zakhidov, Solid State Commun. **60**, 105 (1986).
- ¹⁴D. Bareriswyl, Synth. Met. **41**, 3585 (1991).
- ¹⁵W. P. Su, J. R. Schrieffer, and A. J. Heeger, Phys. Rev. Lett. **42**, 1698 (1979); Phys. Rev. B **22**, 2099 (1980).
- ¹⁶J. A. Blackman and M. K. Sabra, Phys. Rev. B **47**, 15 437 (1993).
- ¹⁷S. J. Xiong, Y. Chen, and S. N. Evangelou, Phys. Rev. Lett. **77**, 4414 (1996).
- ¹⁸D. D. Bradley, Synth. Met. **54**, 401 (1993).
- ¹⁹C. Zhang, D. Braun, and A. J. Heeger, J. Appl. Phys. **73**, 5177 (1993).
- ²⁰Q. Pei and Y. Yang, Chem. Mater. **7**, 1568 (1995).
- ²¹D. Comoretto, Phys. Rev. B **54**, 16 357 (1996).
- ²²H. A. Mizes and E. M. Conwell, Phys. Rev. Lett. **70**, 1505 (1993); Synth. Met. **68**, 145 (1995).
- ²³S. J. Xie, J. Phys.: Condens. Matter **8**, 2185 (1996).
- ²⁴S. J. Xie and L. M. Mei, Phys. Rev. B **47**, 14 905 (1993).
- ²⁵S. J. Xie, J. S. Han, X. D. Ma, L. M. Mei, and D. L. Lin, Phys. Rev. B **51**, 11 928 (1995); Int. J. Mod. Phys. B **11**, 669 (1997).
- ²⁶Y. Furukawa, J. Phys. Chem. **100**, 15 644 (1996).
- ²⁷Y. Uchida, Y. Furukawa, and M. Tasumi, Synth. Met. **69**, 55 (1995).
- ²⁸M. Mauri, W. Graupner, G. Leising, W. Fischer, and F. Sterlzer, Synth. Met. **69**, 73 (1995).